Nonlinear Analysis of Aircraft Loss-of-Control

Harry G. Kwatny[1] and Jean-Etienne T. Dongmo[2] and Bor-Chin Chang[3]
Drexel University, Philadelphia, PA, 19104, USA

Gaurav Bajpai[4] and Murat Yasar[5]
Techno-Sciences, Inc., Beltsville, MD, 20705, USA

Christine Belcastro[6]
NASA Langley Research Center, Hampton, VA, 23681, USA

Loss-of-Control **(LOC) is a major factor in fatal aircraft accidents. Although definitions of LOC remain vague in analytical terms, it is generally associated with flight outside of the normal flight envelope, with nonlinear influences, and with a significantly diminished capability of the pilot to control the aircraft. Primary sources of nonlinearity are the intrinsic nonlinear dynamics of the aircraft and the state and control constraints within which the aircraft must operate. This paper examines how these nonlinearities affect the ability to control the aircraft and how they may contribute to loss-of-control. Specifically, the ability to regulate an aircraft around stall points is considered, as is the question of how damage to control effectors impacts the capability to remain within an acceptable envelope and to maneuver within it. It is shown that even when a sufficient set of steady motions exist, the ability to regulate around them or transition between them can be difficult and nonintuitive, particularly for impaired aircraft. Examples are provided using NASA's Generic Transport Model.**

---

[1] S. Herbert Raynes Professor, MEM Department, Drexel University, 3141 Chestnut Street, Philadelphia, PA, 19104, AIAA Member
[2] Research Associate, MEM Department, Drexel University, 3141, Chestnut Street, Philadelphia, PA, 19104, AIAA Member
[3] Professor, MEM Department, Drexel University, 3141, Chestnut Street, Philadelphia, PA, 19104 ,AIAA Member
[4] Director, Dynamics and Control, Techno-Sciences, Inc., 11750 Beltsville Road, Beltsville, MD, 20705, AIAA Member
[5] Research Engineer, Dynamics and Control, Techno-Sciences, Inc., 11750 Beltsville Road, Beltsville, MD, 20705, AIAA Member
[6] Senior Research Engineer, NASA Langley Research Center, MS 308, Hampton, VA, 23681, AIAA Associate Fellow

Nomenclature

x	State vector
y	Measurements
z	Regulated variables
μ	Bifurcation parameter
u	Control inputs
α	Angle of attack, rad
β	Side slip angle, rad
V	Airspeed, ft/s
X	x inertial coordinate, ft
Y	y inertial coordinate, ft
Z	z inertial coordinate, ft
p	x body-axis angular velocity component, rad/s
q	y body-axis angular velocity component, rad/s
r	z body-axis angular velocity component, rad/s
u	x body-axis translational velocity component, ft/s
v	y body-axis translational velocity component, ft/s
w	z body-axis translational velocity component, ft/s
ϕ	Euler roll angle, rad
θ	Euler pitch angle, rad
ψ	Euler yaw angle, rad
Ψ	Heading, rad
γ	Flight path angle, rad
$\mathbf{p}$	Quasi-velocity vector
$\mathbf{q}$	Generalized coordinate vector
$\mathbf{V}$	Kinematic matrix
$\mathbf{M}$	Inertia matrix
$\mathbf{C}$	Gyroscopic matrix

$\mathbf{F}$ Generalized force vector

C_X Aerodynamic coefficient, force x body axis

C_Y Aerodynamic coefficient, force y body axis

C_Z Aerodynamic coefficient, force z body axis

C_L Aerodynamic coefficient, moment about x body-axis

C_M Aerodynamic coefficient, moment about y body-axis

C_N Aerodynamic coefficient, moment about z body-axis

$C_{\mathcal{D}}$ Aerodynamic drag coefficient, force x wind-axis

$C_{\mathcal{L}}$ Aerodynamic lift coefficient, force z wind-axis

$\bar{c}$ Mean aerodynamic cord, ft

S Reference wing area, ft^2

x_{cg} Center of mass location body x coordinate, ft

x_{cgref} Center of mass reference location body x coordinate, ft

$\hat{\alpha}$ Quasi-static approximation for angle of attack

A System matrix of a linear system

B Control matrix of a linear system

C Output matrix of a linear system

J Jacobian matrix of a multivariable vector function

$\lambda, \tilde{\mathbf{v}}$ Eigenvalue and eigenvector of the Jacobian matrix J

T Thrust, lb

l_t Engine location, z-coordinate, ft

M Aerodynamic moment about y body axis, lbf-ft

m Mass, slugs

I_j Inertia parameters about j-axis, j=x,y,z

g Gravitational constant

ρ air density, lb/ft^3

δ_e Elevator deflection, rad

δ_a Aileron deflection, rad

δ_r Rudder deflection, rad

σ_{min} Minimum singular value

$\mathcal{X}$ State space

$\mathcal{C}$ Envelope

$\mathcal{U}$ Control constraint set

$\mathcal{S}$ Safe set

$\mathcal{T}$ Trim manifold

I. Introduction

RECENT published data shows that during the ten year period 1997-2006, 59% of fatal aircraft accidents were associated with *Loss-of-Control* (LOC) [1]. Yet the notion of loss-of-control is not well-defined in terms suitable for rigorous control systems analysis. The importance of LOC is emphasized in [2] where the inadequacy of current definitions is also noted. On the other hand, flight trajectories have been successfully analyzed in terms of a set of five two-parameter envelopes to classify aircraft incidents as LOC [3]. As noted in that work, LOC is ordinarily associated with flight outside of the normal flight envelope, with nonlinear behaviors, and with an inability of the pilot to control the aircraft. The results in [3] provide a means for analyzing accident data to establish whether or not the accident should be classified as LOC. Moreover, they help identify when the initial upset occurred, and when control was lost. The analysis also suggests which variables were involved, thereby providing clues as to the underlying mechanism of upset. However, it does not provide direct links to the flight mechanics of the aircraft, so it cannot be used proactively to identify weaknesses or limitations in the aircraft or its control systems. Moreover, it does not explain how departures from controlled flight occur. In particular, we would like to know how environmental conditions (like icing) or faults (like a jammed surface or structural damage) impact the vulnerability of the aircraft to LOC.

LOC is essentially connected to the nonlinearity of the flight control problem. Nonlinearity arises in two ways: 1) the intrinsic nonlinearity of the aircraft dynamics, and 2) through state and

control constraints. This paper considers control issues that arise from both sources.

First, the implications of the nonlinear aircraft dynamics are considered. Bifurcation analysis is used to study aircraft control properties and how they change with the flight condition and parameters of the aircraft. The paper extends results previously introduced in [4, 5]. There it was shown that the ability to regulate a system is lost at points associated with bifurcation of the trim equations; ordinarily indicating stall in an aircraft. Such a bifurcation point is always associated with a degeneracy of the zero structure of the system linearization at the bifurcation point. Such degeneracies include loss of (linear) controllability or observability, redundant controls (rank degeneracy of the B matrix) and/or redundant outputs (rank degeneracy of the C matrix). As such points are approached, the ability to regulate degrades so that the performance of the regulator (or pilot) may deteriorate before the bifurcation point is actually reached. The equilibrium surface or set of trim conditions is a submanifold of the state-control-parameter space that is divided into open sets by the bifurcation points. Within each region a linear regulator can be designed. However, a regulator designed in one region will fail if applied in a neighboring region [6]. The key implication of this result is that at the boundary of these sets, i.e., near stall bifurcation points, the strategy required for regulating the aircraft is super-sensitive to parameter variations. Accordingly, we say that the property of regulation is *structurally unstable* at bifurcation points.

Second, the question of how state and control constraints relate to LOC is considered. The Commercial Aviation Safety Team (CAST) defines in-flight LOC as a *significant deviation of the aircraft from the intended flight path or operational envelope* [7]. The flight envelope represents a set of state constraints, so the control issues associated with preventing departure from the constraint set is considered. The notion of a *safe set* [8] or *viable set* [9] is central to this analysis. Suppose an acceptable operating envelope is specified as a domain $\mathcal{C}$ in the state space. The idea of a safe set derives from a decades old control problem in which the plant controls are restricted to a bounded set $\mathcal{U}$ and it is desired to keep the system state within a convex, not necessarily bounded, subset $\mathcal{C}$ of the state space. Feuer and Heyman [10] studied the question: under what conditions does there exist for each initial state in $\mathcal{C}$ an admissible control producing a trajectory that remains in $\mathcal{C}$ for all $t > 0$? When $\mathcal{C}$ does not have this property we try to identify the safe set, $\mathcal{S}$, that is, the largest

subset of $\mathcal{C}$ that does. Clearly, if if it is desired that the aircraft remain in $\mathcal{C}$, it must be insured that it remains in $\mathcal{S}$.

The safe set $\mathcal{S}$ is the largest positively controlled-invariant set contained in $\mathcal{C}$. Safe set theory could be used as a basis for design of envelope protection systems, but this idea has not been fully developed. It is also important to know the extent to which the aircraft can maneuver within $\mathcal{S}$. Controlled flight requires the existence of a suitable set of steady motions and the ability to smoothly transition between them. This means that it is necessary to understand the equilibrium point structure within $\mathcal{S}$ and to identify any impediments to regulating around them or steering from one to another. These questions are examined in this paper.

Ordinarily, if an aircraft is impaired it is to be expected that the safe set will shrink. It will be shown that the equilibrium point structure within the reduced safe set changes as well and the ability to maneuver is significantly diminished. Furthermore, control strategies required to execute transition maneuvers and to regulate around steady motions may be complex and non-intuitive. This may be another mechanism of LOC.

This paper will discuss LOC in terms of controllability/observability, bifurcation analysis, and safe sets analysis. The inter-relationships between these attributes and their relationship to aircraft LOC will be examined. Investigating LOC requires the use of aircraft dynamical models that are accurate outside of the normal flight envelope. In particular it is necessary to characterize post stall and spin behaviors that are often associated with LOC events. Until recently, such models were not available for large transport aircraft. Recent and ongoing work at the NASA Langley Research Center has focused on building aerodynamic models adequate for simulation and analysis in these regimes [11, 12]. A central element in this effort is NASA's Generic Transport Model (GTM) [13] – a 5.5 % dynamically scaled commercial transport model. The GTM will be used to provide analysis examples.

The organization of the paper is as follows. Section II provides a short discussion and literature review of the LOC problem. In Section III the six degrees of freedom GTM mathematical model we use is described. As a simple illustrative example, the phugoid dynamics of the GTM is also employed. This model is also described. Section IV addresses the bifurcation analysis of controlled

dynamical systems. Control issues that arise near stall are specifically addressed. Uncontrolled departures of the GTM near stall are illustrated as well as some first illustrations of recovery from post departure states. In Section VI the safe set and some of its properties are discussed along with examples for unimpaired and impaired aircraft. In Section VII maneuverability is considered and the effects of actuator impairment are illustrated. Finally, Section VIII contains concluding remarks.

II. The Loss-of-Control Problem

Although the majority of fatal aircraft crashes over the past decade or so have been attributed to LOC, its meaning is ambiguous. Generally, a pilot will report LOC if the aircraft does not respond as expected. Consequently, pilot experience can be a major variable in assessing LOC. What LOC is to one pilot may not be to another. Recently, Wilborn and Foster [3] have proposed quantitative measures of LOC. These Quantitative Loss-of-Control (QLC) metrics consist of envelopes defined in two dimensional parameter spaces. Based on the analysis of 24 data sets compiled by the CAST Joint Safety Analysis Team (JSAT) for LOC [7] five envelopes have been defined:

1. *Adverse Aerodynamics Envelope*: (normalized) angle of attack vs. sideslip angle
2. *Unusual Attitude Envelope*: bank angle vs. pitch angle
3. *Structural Integrity Envelope*: normal load factor vs. normalized air speed
4. *Dynamic Pitch Control Envelope*: dynamic pitch attitude ($\theta + \dot{\theta}\Delta t$) vs. % pitch control command
5. *Dynamic Roll Control Envelope*: dynamic roll attitude ($\phi + \dot{\phi}\Delta t$) vs. % lateral control command

The authors provide a compelling discussion of why these envelopes are appropriate and useful. Flight trajectories from the 24 CAST data sets are plotted and the authors conclude maneuvers that exceed three or more envelopes can be classified as LOC, those that exceed two are borderline LOC and normal maneuvers rarely exceed one. According to Ref. [3], the precipitating events of the

CAST LOC incidents were: stalls (45.8%), sideslip-induced rolls (25.0%), rolls from other causes (12.5%), pilot-induced oscillation (12.5%) , and yaw (4.2%).

These results are important. They provide a means for analyzing accident data to establish whether or not the accident should be classified as LOC. Moreover, they help identify when the initial upset occurred, when control was lost and suggest which variables were involved. However, because the approach does not directly connect to the flight mechanics of the aircraft, it does not identify weaknesses or limitations in the aircraft or its control systems. Moreover, it does not explain how departures from controlled flight occur. In particular, we would like to know how environmental conditions or actuator failures or structural damage impact the vulnerability of the aircraft to LOC. To do this we need a formal analytical definition of LOC.

Another important study [2] reviews 74 transport LOC accidents in the fifteen year period 1993-2007. Of these the major underlying causes of LOC are identified as stalls, ice contaminated airfoils, spatial disorientation, and faulty recovery technique.

A recent study [14] goes further, investigating 126 LOC accidents that span three decades from 1979-2009. Accident reports were used to identify fourteen *causal* and *contributing* events. These fourteen events are grouped into three broad categories:

1. Adverse onboard conditions

2. External hazards and disturbances

3. Vehicle upsets

The analysis identifies six events divided amongst these categories as the most significant contributors to LOC incidents in terms of the number of fatalities: Category 1 – System Faults/Failures/Errors, Vehicle Impairment/Damage, Inappropriate Crew Response; Category 2 – Atmospheric Disturbances related to Wind Shear/Gusts, and Snow/Icing; Category 3 – Stall/Departure from controlled flight.

Most importantly, the authors note that almost all LOC incidents involve a sequence of events. They observe that vehicle upsets are rarely the precipitating factor in the LOC sequence, but most LOC sequences include *vehicle upset* somewhere in the chain of events. Vehicle upset category

includes five events:

1. Abnormal attitude
2. Abnormal airspeed, abnormal angular rates, asymmetric forces
3. Abnormal flight trajectory
4. Uncontrolled descent
5. Stall, departure from controlled flight

Of these, Stall/departure is clearly the most prevalent. The prevalence of stalls in LOC incidents suggests the importance of bifurcation behavior as a factor in LOC. We discuss this further in Section IV.

An aircraft must operate in multiple modes that have significantly different dynamics and control characteristics; for example, cruise and landing configurations. Within each mode there may be some parametric variation, such as weight or center of mass location, that also affects aircraft behavior. Each mode has associated with it a flight envelope restricting speed, attitude and other flight variables. Under normal conditions keeping within the flight envelope provides sufficient maneuverability to perform the mode mission while insuring structural integrity of the vehicle for all admissible parameter variations and all anticipated disturbances. Abnormal conditions, e.g., icing, faults or damage, will alter aircraft dynamics and may require the definition of a new mode with its own flight envelope.

Ordinarily a flight envelope can be considered a convex polyhedral set, not necessarily bounded, in the state space. Thus, the aircraft needs to operate within the state constraints imposed by the envelope. Insuring that an aircraft remains within its flight envelope is called *envelope protection*. Envelope protection is generally the responsibility of the pilot but there is an increasing interest in the use of automatic protection systems [15–18], although these are not foolproof.

Because the controls themselves as well as the states are constrained, the question of whether it is even possible to keep the aircraft within the envelope is not trivial. Questions like this have been considered in the control literature [8, 9, 19–22]. In Section VI below we discuss the problem

of identifying the largest set within a prescribed envelope that can be made positively invariant and of characterizing the control strategy necessary to do so. This set will be called the *safe set*. It is possible to be inside of the envelope and yet outside of the safe set. In which case it is impossible, no matter how clever the pilot or the control system, to keep the aircraft within its flight envelope. In a strict sense departure from the safe set implies LOC. It may, of course, be possible to employ a recovery strategy to restore the system to the safe set. So an aircraft may be out of control and yet recoverable. Indeed, there it is generally believed that most unimpaired transport aircraft are recoverable if timely remedial action is initiated.

Besides the control bounds, other restrictions may be placed on the admissible controls that could further restrict the safe set. For instance, we could require that only smooth feedback controls be employed. These and related issues will be discussed below.

III. Dynamics of the GTM

In the subsequent discussion we will provide examples based on NASA's Generic Transport Model (GTM). Data obtained from NASA have been used to develop symbolic and simulation models. Nonlinear symbolic models are used to perform bifurcation analysis and nonlinear control analysis and design. Linear Parameter Varying (LPV) models are derived from the nonlinear symbolic model and have been used to study the variation in the structure of the linear control system properties around bifurcation points. Simulation models are also automatically assembled from the symbolic model in the form of optimized C-code that compiles as a MEX file for use as an S-function in Simulink. The GTM model is described in Section III A.

In addition to the full six degrees of freedom model, we will also present examples using only the phugoid dynamics of the GTM. Besides being a useful example in its own right, it has the distinct advantage for us in that it has a two dimensional state space allowing us to provide simple graphical illustrations of complex general principles. In Section III B we describe the model.

A. The Generic Transport Model

The six degrees of freedom aircraft model has 12 or 13 states depending on whether we use Euler angles or quaternion for attitude characterization. In the Euler angle case the model is generated

in the form of Poincaré's equations [23],

$$\dot{\mathbf{q}} = \mathbf{V}(\mathbf{q})\,\mathbf{p} \tag{1}$$

$$\mathbf{M}(\mathbf{q})\,\dot{\mathbf{p}} + \mathbf{C}(\mathbf{q},\mathbf{p})\,\mathbf{p} + \mathbf{F}(\mathbf{p},\mathbf{q},\mathbf{u}) = 0 \tag{2}$$

where $\mathbf{q} = (\phi, \theta, \psi, X, Y, Z)^T$ is the generalized coordinate vector, $\mathbf{p} = (p, q, r, u, v, w)^T$ is the quasi-velocity vector. Alternatively, it is sometimes necessary to replace the Euler angles ϕ, θ, ψ with the quaternion q_0, q_1, q_2, q_3. The key parameters in the formulation are: the kinematic matrix $\mathbf{V}(\mathbf{q})$, the inertia matrix $\mathbf{M}(\mathbf{q})$, the gyroscopic matrix $\mathbf{C}(\mathbf{q},\mathbf{p})$. The force function $\mathbf{F}(\mathbf{p},\mathbf{q},\mathbf{u})$ includes all of the aerodynamic, engine and gravitational forces and moments. Ultimately the engine and aerodynamic forces depend on the control inputs $\mathbf{u}$. We can combine the kinematics (1) and dynamics (2) to obtain the state equations

$$\dot{x} = f(x, u, \mu) \tag{3}$$

where $\mu \in R^k$ is an explicitly identified vector of distinguished aircraft parameters such as mass or center of mass location (or even set points for regulated variables), $x \in R^n$ is the state vector, and $u \in R^m$ is the control vector. In the Euler angle case, $n = 12$ and the state is given by $x = [\phi, \theta, \psi, X, Y, Z, p, q, r, u, v, w]^T$. There are 4 control inputs, given by $u = [T, \delta_e, \delta_a, \delta_r]^T$. The controls are limited as follows: thrust $0 \leq T \leq 40$ lbf, elevator $-40^\circ \leq \delta_e \leq 20^\circ$, aileron $-20^\circ \leq \delta_a \leq 20^\circ$, and rudder $-30^\circ \leq \delta_r \leq 30^\circ$. Velocity is in ft/s.

Aerodynamic models were obtained from NASA. They are based on data obtained with a 5.5 % scale model in the NASA Langley 14 ft $\times$ 22 ft wind tunnel as described in [12]. Aerodynamic force and moment coefficients are generated using a multivariate orthogonal function method as described in [24, 25]. In the original NASA model several regions of angle of attack were used to capture severe nonlinearity. These models were blended using Gaussian weighting. For simplicity we use only one of the models for the analysis herein.

B. The Phugoid Model

The longitudinal dynamics of a rigid aircraft can be easily derived from the six degrees of freedom model by restricting motion to the longitudinal variables. When written in flight path

coordinates the longitudinal model takes the form:

$$\begin{aligned}
\dot{\theta} &= q \\
\dot{x} &= V\cos\gamma \\
\dot{z} &= V\sin\gamma \\
\dot{V} &= \tfrac{1}{m}\left(T\cos\alpha - \tfrac{1}{2}\rho V^2 S C_{\mathcal{D}}\left(\alpha,\delta_e,q\right) - mg\sin\gamma\right) \\
\dot{\gamma} &= \tfrac{1}{mV}\left(T\sin\alpha + \tfrac{1}{2}\rho V^2 S C_{\mathcal{L}}\left(\alpha,\delta_e,q\right) - mg\cos\gamma\right) \\
\dot{q} &= \tfrac{M}{I_y}, \quad M = \left(\tfrac{1}{2}\rho V^2 S\bar{c} C_M\left(\alpha,\delta_e,q\right) + \tfrac{1}{2}\rho V^2 S\bar{c} C_Z\left(\alpha,\delta_e,q\right)\left(x_{cgref} - x_{cg}\right) - mgx_{cg} + l_t T\right) \\
\alpha &= \theta - \gamma
\end{aligned} \tag{4}$$

A classic analysis problem of aeronautics was introduced by Lanchester [26] over one hundred years ago – the long period *phugoid* motion of an aircraft in longitudinal flight. The phugoid motion is a roughly constant angle of attack behavior involving an oscillatory pitching motion with out of phase variation of altitude and speed. The phugoid mode is the primary mode to be regulated during landing and it is often unstable. The ability to stabilize the phugoid motion using the elevator or thrust is important and ordinarily quite easy for unimpaired aircraft. The inability to do so, however, has been linked to a number of fatal airline accidents including Japan Airlines Flight 123 in 1985 and United Airlines Flight 232 in 1989 [27].

We will illustrate several computations by examining the controlled phugoid dynamics of the GTM. The problem is similar to one considered in [9, 28] to illustrate safe set computations. The key assumption is that pitch rate rapidly approaches zero so that the the phugoid motion is characterized by $q \equiv 0$. Thus, we must have

$$M = \left(\tfrac{1}{2}\rho V^2 S\bar{c} C_M\left(\alpha,\delta_e,q\right) + \tfrac{1}{2}\rho V^2 S\bar{c} C_Z\left(\alpha,\delta_e,q\right)\left(x_{cgref} - x_{cg}\right) - mgx_{cg} + l_t T\right) = 0 \tag{5}$$

From equation (5) we obtain a quasi-static approximation for the angle of attack

$$\alpha = \hat{\alpha}\left(V, T, \delta_e\right) \tag{6}$$

so that the $V-\gamma$ equations in (4) decouple from the remaining equations. Thus, we have a closed system of two differential equations that define the phugoid dynamics:

$$\begin{aligned}
\dot{V} &= \tfrac{1}{m}\left(T\cos\hat{\alpha} - \tfrac{1}{2}\rho V^2 S C_{\mathcal{D}}\left(\hat{\alpha},\delta_e,0\right) - mg\sin\gamma\right) \\
\dot{\gamma} &= \tfrac{1}{mV}\left(T\sin\hat{\alpha} + \tfrac{1}{2}\rho V^2 S C_{\mathcal{L}}\left(\hat{\alpha},\delta_e,0\right) - mg\cos\gamma\right)
\end{aligned} \tag{7}$$

The angle of attack, α can be considered as an output as given by equation (5).

We specify an operating envelope

$$\mathcal{C} = \{(V, \gamma) \,|90 \text{ f/s} \leq V \leq 240 \text{ f/s}, -22^\circ \leq \gamma \leq 22^\circ \}$$

and control restraint set

$$\mathcal{U} = \{(T, \delta_e) \,|0 \leq T \leq 40 \text{ lbf}, -40^\circ \leq \delta_e \leq 20^\circ \}$$

IV. Aircraft Trim and Bifurcation Analysis

Departures from controlled flight like stall and spin have concerned aircraft engineers from the earliest days of flight. In recent years departure has been analyzed by using a combination of simulation and flight test (with manned aircraft or scale models - see, for example, the informative report [29]). An example, that may be considered 'state-of-the-art' for studies of this type, concerns the falling leaf and related behaviors of the F-18 [30–32]. Only in the past two decades have formal methods of bifurcation analysis been applied to aircraft [4, 33–42]. Bifurcation analysis has been employed to identify the conditions for occurrence of undesirable behaviors, to investigate recovery methods from dangerous post bifurcation modes and to formulate feedback control systems that modify bifurcation behavior.

In this paper the regulation of aircraft to a desired trim condition is considered. In general the equations of motion of a rigid aircraft involve six degrees of freedom involving the six coordinates $\phi, \theta, \psi, X, Y, Z$ and six quasi-velocities p, q, r, u, v, w. If the change in density with altitude variation is ignored and the atmosphere is assumed still, then the dynamics are invariant with respect to (X, Y, Z) and ψ. Consequently, in the study of steady motions it is usual to ignore the inertial location and also yaw, and consider only the six velocities and pitch and roll of the vehicle. The reduced dynamics comprise an eight dimensional system of state equations ($n = 8$) that are nonlinear and may be parameter dependent. Of concern are steady motions that can be defined in terms of these variables. In particular, these motions are trajectories in inertial space, that can be associated with equilibria of the eight state system. It is important to know whether or not it is possible to regulate to and steer along these motions. This naturally leads to the study of the existence and stabilizability of equilibria of the reduced nine state system.

It is important to emphasize that most applications of bifurcation analysis to aircraft view the aircraft as a *dynamical system* in which the control inputs are treated as the bifurcation parameters. In this work, as in [4], the system is viewed as a *control system*, that is, a dynamical system with an input-output structure as well as parameters. Consequently the bifurcation points are linked with control system properties like controllability and observability rather than stability. This gives a unique view of how operation near bifurcation points impacts the ability to control the aircraft.

A. Trim conditions

The idea of aircraft trim is so broadly entrenched that one would assume it requires no further discussion. However, there are subtleties that need to be explored. A general formulation is as follows. Assume the aircraft is described by the state equations in the form of (1) and (2), or (3).

Definition 1. Steady Motion A *steady motion* is one for which all 6 velocities are constant, i.e., $\dot{u} = 0, \dot{v} = 0, \dot{w} = 0$, (equivalently, $\dot{V} = 0,\ \dot{\alpha} = 0, \dot{\beta} = 0$) and $\dot{p} = 0, \dot{q} = 0,\ \dot{r} = 0$. From (2), with $\dot{\mathbf{p}} = 0$,

$$g\left(x, u, \mu\right) := C\left(\mathbf{q}\right)\mathbf{p} + F\left(\mathbf{p}, \mathbf{q}, \mathbf{u}\right) = 0 \tag{8}$$

The steady motion requirement, (8), provides six equations to which we add a set of $n + m - 6$ *trim* equations:

$$h\left(x, u, \mu\right) = 0 \tag{9}$$

Equations (8) and (9) form a set of $n + m$ equations in $n + m + k$ variables. Ordinarily we fix the k parameters, μ, and solve for the remaining $n + m$ variables – the state x and the control u.

Definition 2. Trim Point Given the steady motion equation (8), the trim condition (9), an envelope $\mathcal{C}$ and a control restraint set $\mathcal{U}$, a *viable trim point* or simply a *trim point*, with respect to the fixed parameter μ is a pair (x, u) that satisfies (8) and (9) and also $x \in \mathcal{C}$, $u \in \mathcal{U}$. The set of viable trim points is called the *trim set*, $\mathcal{T}$.

The important point is that for a prescribed trim condition (9) there are often multiple viable trim points. The general study of the trim point structure as a function of the parameters is a

problem of static bifurcation analysis [4, 43–46]. When $k = 1$ this can be carried out using a continuation method. Let us consider two examples of the trim condition for the model described in Section III. In this case there are eight states ($n = 8$) and four controls ($m = 4$). Thus, six trim conditions are required. First consider straight wings-level flight:

1. speed, $V = V^*$
2. constant roll, pitch and heading, $\dot{\phi} = 0, \dot{\theta} = 0, \dot{\psi} = 0$
3. roll angle, $\phi = 0$
4. flight path angle, $\sin\gamma^* + \cos\theta\left(\cos\beta\cos\phi\sin\alpha + \sin\beta\sin\phi\right) - \cos\alpha\cos\beta\sin\theta = 0$

Second, consider a coordinated turn. In this case the aircraft rotates at constant angular velocity, ω^* about the inertial z-axis. Thus the attitude of the aircraft varies periodically with time.

1. speed, $V = V^*$
2. coordinated turn condition, $pV\cos\beta\sin\alpha - rV\cos\beta\cos\alpha + g\cos\theta\sin\phi = 0$
3. angular velocity, $p = -\omega^*\sin\theta, q = \omega^*\cos\theta\sin\phi, r = \omega^*\cos\theta\cos\phi$
4. flight path angle, $\sin\gamma^* + \cos\theta\left(\cos\beta\cos\phi\sin\alpha + \sin\beta\sin\phi\right) - \cos\alpha\cos\beta\sin\theta = 0$

Here is a simple example of trim points for the phugoid model.

Example 1. Trim Points of the Phugoid Model This example examines the trim motions associated with a specified speed and flight path angle. In accordance with (7), with V and γ specified, it is necessary to find T and δ_e such that

$$\begin{aligned} 0 &= T\cos\hat{\alpha} - \tfrac{1}{2}\rho V^2 S C_{\mathcal{D}}\left(\hat{\alpha}, \delta_e, 0\right) - mg\sin\gamma \\ 0 &= T\sin\hat{\alpha} + \tfrac{1}{2}\rho V^2 S C_{\mathcal{L}}\left(\hat{\alpha}, \delta_e, 0\right) - mg\cos\gamma \end{aligned} \tag{10}$$

As an example, consider steady flight with $\gamma = 0$ and various speeds, V, – yielding a one-parameter problem. Beginning with the trim condition: $V = 150$ fps, $\gamma = 0$ deg, $T = 4.0991$ lbf, $\delta_e = 1.725$ deg perform a continuation analysis to obtain the results in Figure 1. The corresponding initial value for angle of attack is $\alpha = 2.96644$ deg.

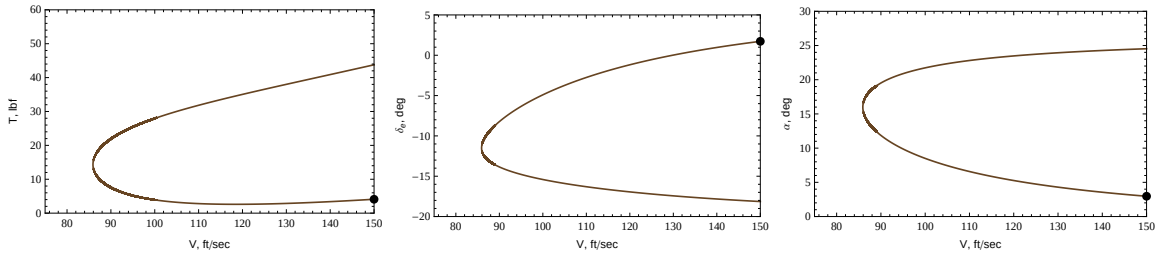

(a) Thrust (b) Elevator Position (c) Angle of Attack

Fig. 1 The figure shows the trim values for thrust, elevator and angle of attack for various values of airspeed, V, and $\gamma = 0$. Note that the starting point for the continuation is identified by the black dot.

Starting at the black dot, as airspeed drops the trim points follow the lower branch of the thrust and angle of attack curves and the upper branch of the elevator curve until the bifurcation (stall) point is reached ($V = 85.9150$ fps, $T = 14.3440$ lbf, $\delta_e = -11.5059$ deg). These are the 'normal' trim points, but the alternate branch is also comprises viable trim points so long as the thrust and elevator are within bounds. This observation can be important, as we will see below. We might refer to these as *high angle of attack* trim points.

It should be noted that the GTM has a thrust to weight ratio that is much higher than a typical transport aircraft. Thus, the high speed, high angle of attack trims are not likely to be viable in a typical transport.

B. Control issues at stall

Consider a parameter dependent, nonlinear control system given by

$$\begin{aligned} \dot{x} &= f(x, u, \mu) \\ z &= h(x, \mu) \end{aligned} \tag{11}$$

where $x \in R^n$ are the states, $u \in R^m$ are the control inputs, $z \in R^r$ are the regulated variables and $\mu \in R$ is any parameter. Assume that f, h are smooth (sufficiently differentiable). The parameter could be a physical variable like the weight of the aircraft or the center of gravity location; or a regulated variable like velocity, flight path angle, altitude or roll angle; or the position of a stuck control surface. The regulator problem is solvable only if $p \geq r$. Since the number of controls can

always be reduced, henceforth assume $p = r$.

A triple $(x^\star, u^\star, \mu^\star)$ is an *equilibrium point* (or trim point) of (11) if

$$F(x^\star, u^\star, \mu^\star) := \begin{pmatrix} f(x^\star, u^\star, \mu^\star) \\ \\ h(x^\star, \mu^\star) \end{pmatrix} = 0 \tag{12}$$

The *equilibrium surface* is the set $\mathcal{E} = \left\{(x, u, \mu) \in R^{n+m+k} \,|F\,(x, u, \mu) = 0\right\}$.

Definition 3. (from [4]) An equilibrium point $(x^\star, u^\star, \mu^\star)$ is *regular* if there is a neighborhood of $\mu^\star$ on which there exist unique, continuously differentiable functions $\overline{x}(\mu)$, $\overline{u}(\mu)$ satisfying

$$F(\overline{x}(\mu), \overline{u}(\mu), \mu) = 0 \tag{13}$$

If an equilibrium point is not a regular point it is a *bifurcation point.*

Stall is typically discussed in connection with a single airfoil where it is associated with a reduction in lift when the angle of attack exceeds a critical value. In fixed wing aircraft stalls are induced by reducing airspeed and compensating for the consequent reduced lift by increasing the angle of attack. Ultimately, the force and moment balances cannot be maintained and the aircraft stalls. The airspeed at which this collapse occurs is called the stall (or stalling) speed. Stall can occur in various aircraft configurations, during steady climbs or descents, and while flying straight and level or in banked turns. More formally, *stall speed* is typically defined as *the minimum steady flight speed obtainable in a specific configuration* or *the minimum controllable steady flight speed in a specific configuration.* While these definitions do convey the meaning of stall, they can be ambiguous because the terms 'obtainable' and 'controllable' are not precisely defined. For the purposes of this discussion the following definition is employed.

Definition 4. Consider a one dimensional trim set in which the single parameter μ is the airspeed, V. A *stall point* is a viable trim point that is also a bifurcation point of the trim equations.

As will be seen, this definition does capture the definitions of stall speed as noted above and, it is precise and applicable in more general situations.

The Implicit Function Theorem implies that an equilibrium point is a bifurcation point only if $\det J = 0$. The Jacobian J is given by

$$J = [D_x F(x^\star, u^\star, \mu^\star) \quad D_u F(x^\star, u^\star, \mu^\star)] \tag{14}$$

Now, if A, B, C, D denotes the linearization at $(x^\star, u^\star, \mu^\star)$ of (11) with output z so that

$$J = \begin{bmatrix} A & B \\ C & 0 \end{bmatrix}$$

then we have the following theorem for a static bifurcation point.

Theorem 1 *(from [4]) An equilibrium point $(x^\star, u^\star, \mu^\star)$ is a static bifurcation point only if*

$$Im \begin{pmatrix} A & B \\ C & 0 \end{pmatrix} \neq R^{n+r} \tag{15}$$

Recall that the system matrix is

$$P(\lambda) = \begin{pmatrix} \lambda I - A & B \\ -C & 0 \end{pmatrix}$$

From this observation, *necessary* conditions for a static bifurcation point can be obtained as follows [5]:

Theorem 2 *The equilibrium point $(x^\star, u^\star, \mu^\star)$ is a static bifurcation point of (11) only if one of the following conditions is true for its linearization:*

1. *there is a transmission zero at the origin,*
2. *there is an uncontrollable mode with zero eigenvalue,*
3. *there is an unobservable mode with zero eigenvalue,*
4. *it has insufficient independent controls,*
5. *it has redundant regulated variables.*

The key implication of this theorem is that the ability to locally regulate the system diminishes as the bifurcation point is approached [6, 47]. In fact a linear regulator (indeed a smooth feedback regulator) does not exist at the bifurcation point [4]. At the bifurcation point an arbitrarily small perturbation of parameters changes the zero structure of the system thereby requiring a fundamental change in the controller [6]. The point we wish to emphasize is that losing the capacity to regulate nonlinear flight dynamics is intimately connected to the bifurcation structure of the trim equations

of the aircraft. Thus, at least some forms of LOC can be rigorously connected to the flight dynamics. This argument is also made very strongly in [39].

Example 2. Regulating Trim Motions of the Phugoid Dynamics An essential point is that the control behaviors around trim points on the two branches, see Figure 1, are considerably different so that a strategy to regulate around a point on one branch will fail if applied to one on the other branch. The theoretical basis for this is established in [4, 6, 47, 48] as summarized above. Here is a simple example. Consider the two trim points at 90 fps, the *normal trim point*, $V = 90$ fps, $\gamma = 0$ deg, $T = 7.58222$ lbf, $\delta_e = -8.22916$ deg and the *high angle of attack trim point*, $V = 90$ fps, $\gamma = 0$ deg, $T = 21.9189$ lbf, $\delta_e = -13.8494$ deg. The linear dynamics at each of these trim points is, first for the normal trim:

$$\frac{d}{dt}\begin{bmatrix}\Delta V\\ \Delta\gamma\end{bmatrix} = \begin{bmatrix}-0.186044 & -33.2125\\ 0.008844275 & 0.0150152\end{bmatrix}\begin{bmatrix}\Delta V\\ \Delta\gamma\end{bmatrix} + \begin{bmatrix}0.449195 & 62.3033\\ 0.00416546 & -0.751226\end{bmatrix}\begin{bmatrix}\Delta T\\ \Delta\delta_e\end{bmatrix}$$

and for the high angle of attack trim:

$$\frac{d}{dt}\begin{bmatrix}\Delta V\\ \Delta\gamma\end{bmatrix} = \begin{bmatrix}-0.310011 & -33.2514\\ 0.00638713 & -0.0338864\end{bmatrix}\begin{bmatrix}\Delta V\\ \Delta\gamma\end{bmatrix} + \begin{bmatrix}0.494357 & 31.5244\\ -0.00127241 & 1.22673\end{bmatrix}\begin{bmatrix}\Delta T\\ \Delta\delta_e\end{bmatrix}$$

Inspection of the control input matrix shows the reversal of the effect of the elevator, δ_e. At the normal trim a positive (counterclockwise) rotation of the elevator causes a reduction of the flight path angle, i.e., pitch down. On the other hand, at the high angle attack trim a positive elevator rotation causes an increase in flight path angle. This behavior is, of course, well known [49], p. 612.

This behavior is organized by the singular zero dynamics at the bifurcation point that separates the two branches. The state equations linearized at the bifurcation point are

$$\frac{d}{dt}\begin{bmatrix}\Delta V\\ \Delta\gamma\end{bmatrix} = \begin{bmatrix}-0.27235 & -33.8550\\ 0.00791414 & -0.00286013\end{bmatrix}\begin{bmatrix}\Delta V\\ \Delta\gamma\end{bmatrix} + \begin{bmatrix}0.400642 & 62.5119\\ 0.00170008 & 0.265262\end{bmatrix}\begin{bmatrix}\Delta T\\ \Delta\delta_e\end{bmatrix}$$

Inspection of the two columns of the control input matrix shows that they are dependent – the second obtained from the first by multiplication by 156.029. Thus, the controls are redundant. There is only one effective control direction. The important implication is that, from a linear perspective, both V and γ cannot be simultaneously regulated [50]. Another indication of the degeneracy of the linearized

system at the bifurcation point is the degeneracy of the transfer matrix, $G(s)$, $(T, \delta_e) \to (V, \gamma)$:

$$G(s) = \frac{1}{s^2 + 0.27521s + 0.268712} \begin{bmatrix} 0.400642s - 0.0564101 & 62.5119s - 8.80163 \\ 0.001700086 + 0.00363376 & 0.265262s + 0.566973 \end{bmatrix}$$

A simple computation shows that $|G(s)| \equiv 0$.

Finally, as a separate observation from Figure 1 (a), note that as stall is approached with decreasing airspeed thrust must be increased. Thus there is a reversal from the normally anticipated increase of thrust with increasing airspeed.

V. Control Behavior of the GTM Near Stall

In this section the goal is to illustrate the control behavior of the GTM around trim points near stall. First, uncontrolled departures from controlled flight near stall bifurcation points are examined. Then controllability change as stall is approached is illustrated. Finally, some brief remarks about recovery from departures near stall are given.

A. Uncontrolled departures near stall: GTM example

Simulated GTM departures from a coordinated turn at various speeds near the stall speed are considered. In each case the aircraft is trimmed very near a coordinated turn equilibrium condition. The controls are then fixed and the resultant trajectories are observed. Below results for three speeds – 90 ft/sec, 87 ft/sec, and 85 ft/sec are shown. The last is very close to the stall speed. See Figure 2. The equilibrium surface was generated as a function of airspeed using a continuation method as described in [45]. Projections of this surface are shown in Figure 2 which shows angle of attach α, elevator deflection δ_e, aileron deflection δ_a, and thrust T as functions of airspeed V. The points selected for simulation are identified in the figure.

Figures 3 on page 22 and 4 on page 23 present a snapshot of the results. The former shows the ground tracks and adverse aerodynamics plots. The latter displays the aircraft attitude in terms of the Euler angles.

At 90 ft/sec the aircraft cleanly enters the coordinated turn. At 87 ft/sec, closer to stall speed, it departs from trim and within 20 seconds enters a well-formed, slowly descending, periodic motion

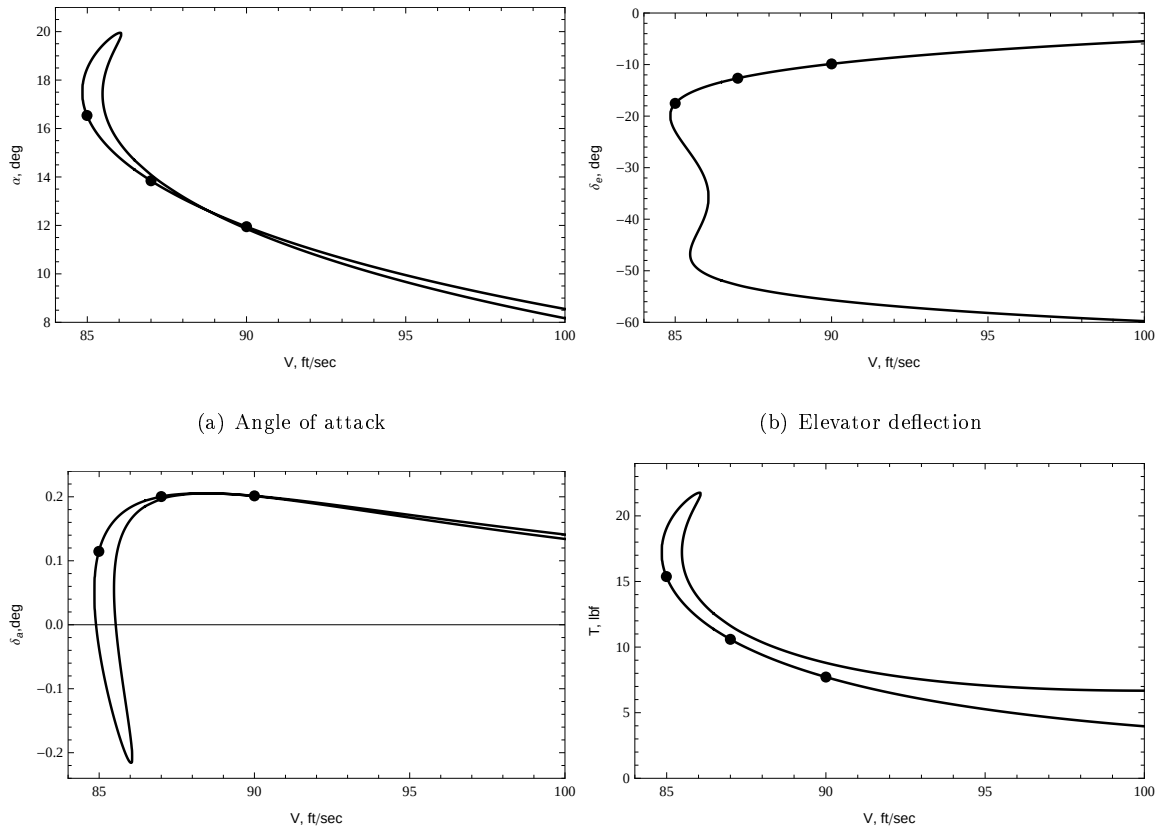

(a) Angle of attack

(b) Elevator deflection

(c) Aileron deflection

(d) Thrust

Fig. 2 Projections of the coordinated turn equilibrium surface shows angle of attack, elevator deflection, aileron deflection and thrust as functions of the parameter airspeed.

with rather violent swings in attitude, particularly roll. Near stall speed, at 85 ft/sec, the vehicle departs from trim and enters a steeply descending, apparently chaotic motion with increasingly violent attitude swings. The simulation model utilizes a quaternion representation of attitude from which the Euler angles are computed. These are displayed in Figure 4.

As described in [3], the angle of attack versus sideslip angle plot, i.e., the Adverse Aerodynamics Envelope, is a useful indicator of LOC. The simulation results are shown in Figure 3 on the following page. We see the well contained data set for 90 ft/sec, and even for 87 ft/sec. However, the stall departure case, 85 ft/sec, suggests a serious control problem although this trajectory is obtained with fixed controls. This is consistent with the observations in Section IV B.

With reference to Figure 4 (c) the large roll angles and roll rates suggest that other LOC indicators identified in [3] are also triggered – specifically, the Unusual Attitude envelope.

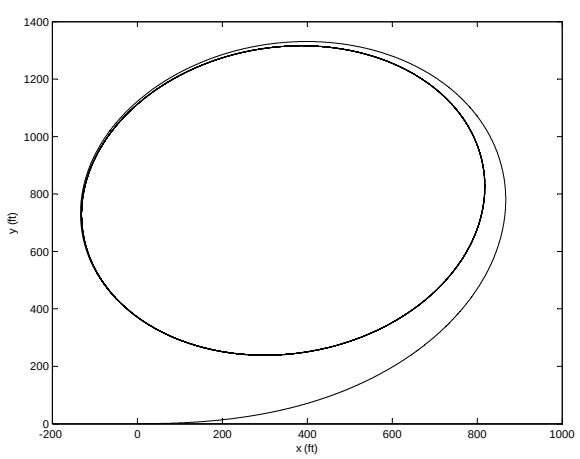

(a) 90 ft/sec

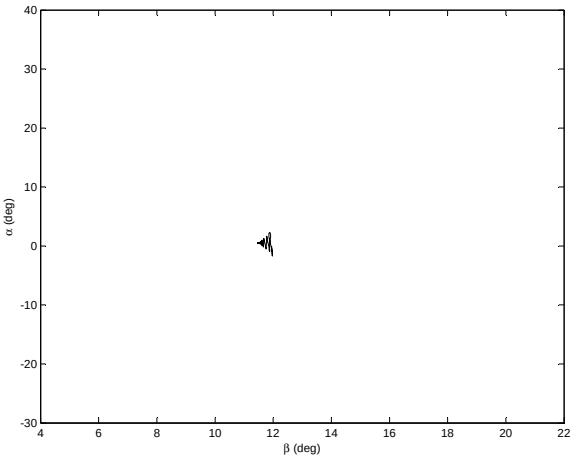

(b) 90 ft/sec

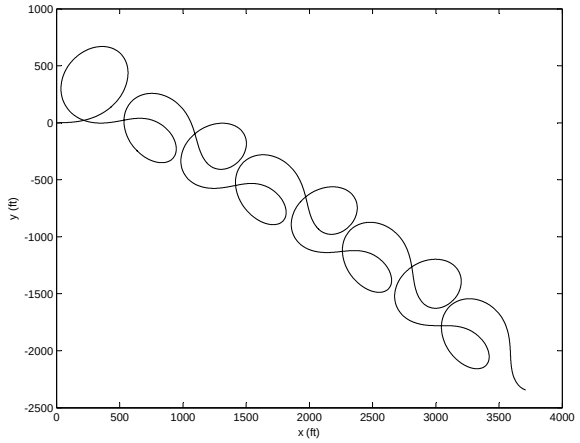

(c) 87 ft/sec

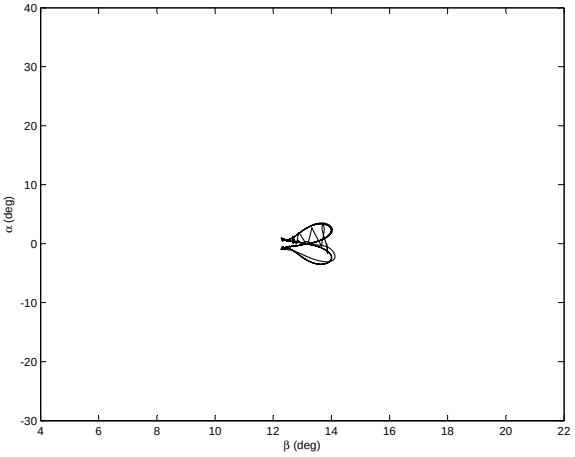

(d) 87 ft/sec

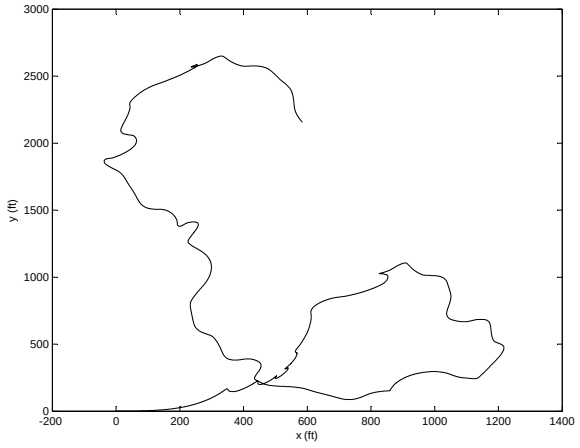

(e) 85 ft/sec

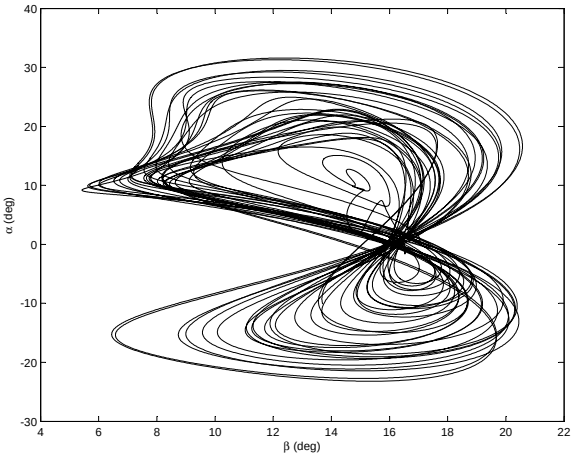

(f) 85 ft/sec

Fig. 3 Coordinated turn ground tracks and adverse aerodynamics plots: at 90 ft/sec the the aircraft stabilizes in a coordinated turn; at 87 ft/sec, closer to stall speed, the aircraft departs from the coordinated turn and enters a periodic motion much like an extremely exaggerated Dutch roll; at 85 ft/sec, approximately stall speed, the aircraft departs to an erratic motion, possibly chaotic.

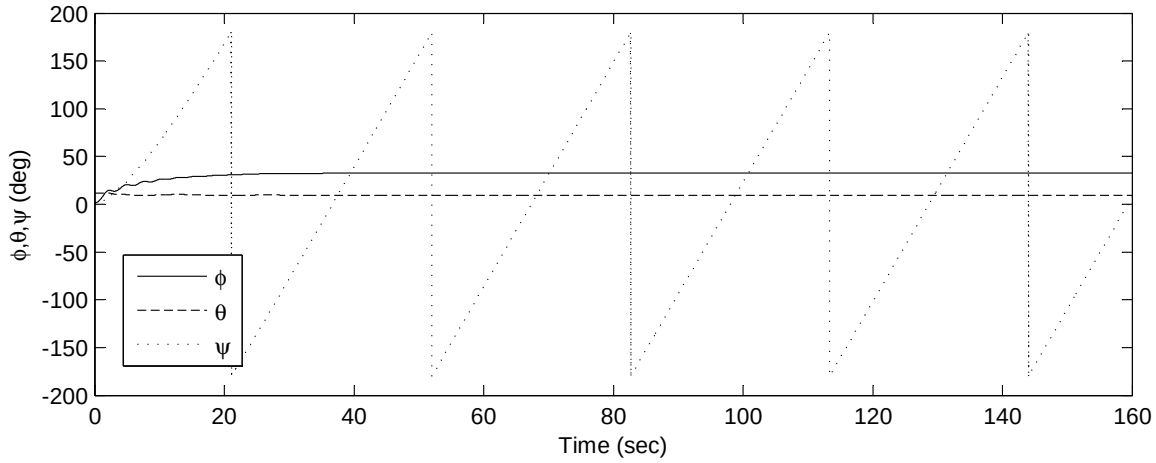

(a) 90 ft/sec

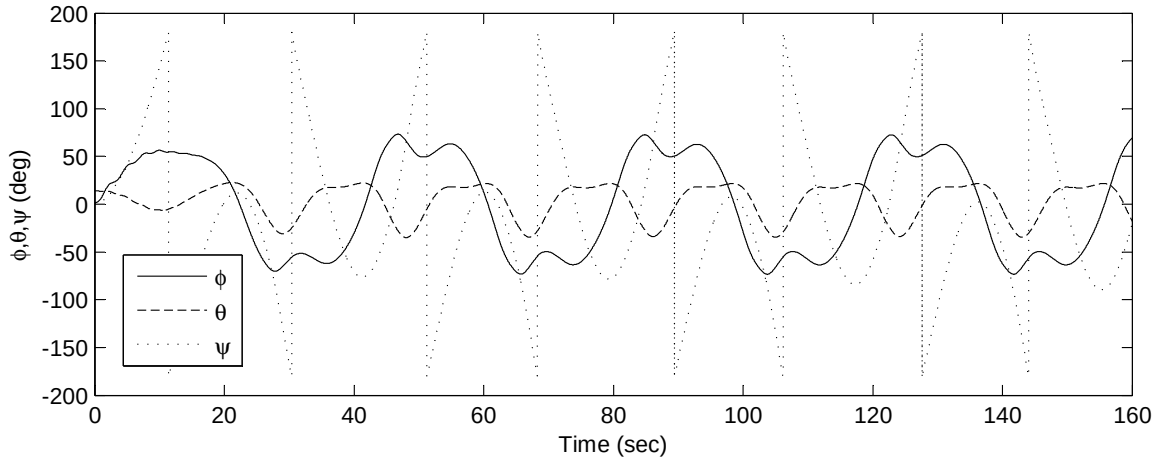

(b) 87 ft/sec

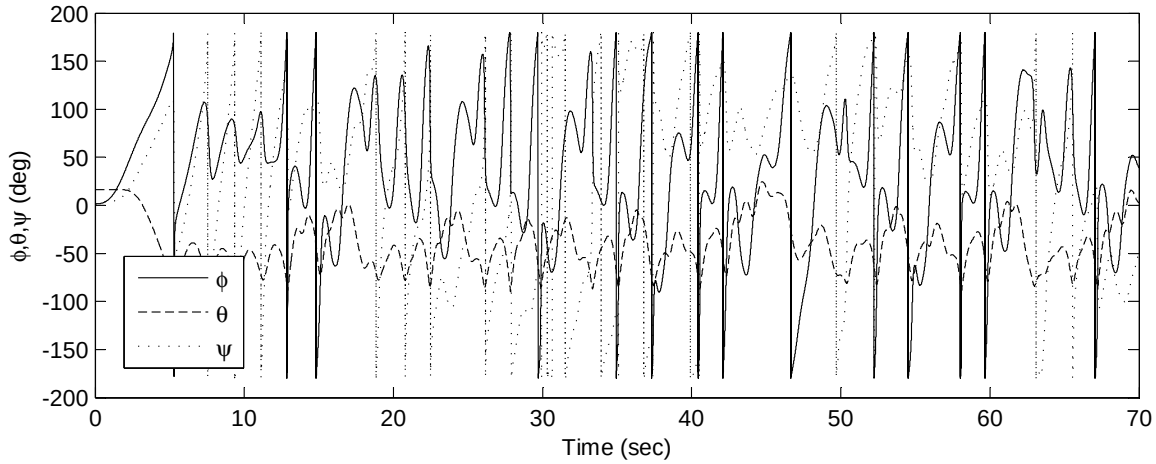

(c) 85 ft/sec

Fig. 4 Coordinated turn attitude. (a) at 90 ft/sec the attitude stabilizes as expected. (b) at 87 ft/sec the aircraft enters a periodic trajectory. (c) at 85 ft/sec, approximately stall speed, the aircraft departs to an erratic motion.

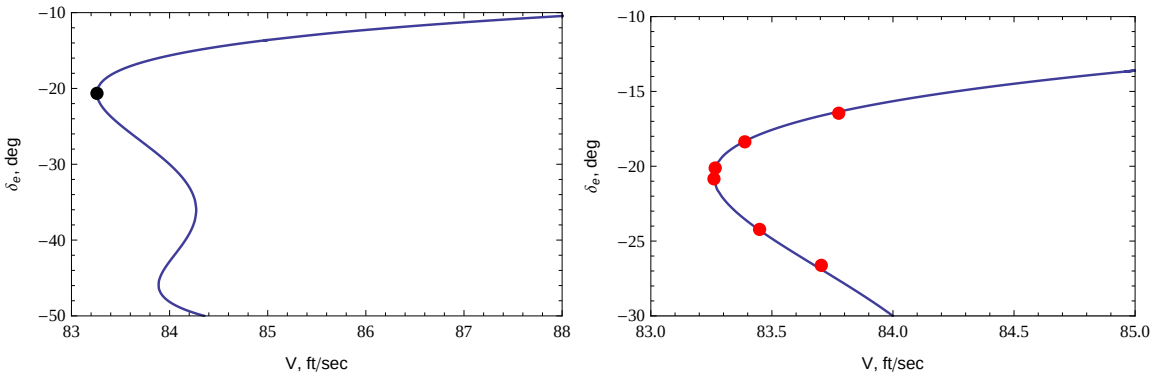

(a) Bifurcation point.

(b) Other equilibria.

Fig. 5 The equilibrium curve is shown for straight, wings level climb with speed as the parameter. The stall point is indicated in (a). A two parameter LPV model is derived around the bifurcation point with parameters speed and flight path angle. This involves deriving a polynomial approximation to the equilibrium surface around the bifurcation point (see [51]). In (b) several points computed from the approximating surface are compared to the actual surface.

B. Control properties around the bifurcation point: GTM example

In accordance with Theorem 2 some degeneracy in the linear system zero dynamics at the bifurcation point is anticipated. To illustrate this, again consider the GTM, this time in a straight, wings level climb with flight path angle of 0.1 rad (5.7 deg). The equilibrium points are plotted as a function of speed in Figure 5. Now, a two-parameter family of linear systems (LPV model) is constructed using the method described in [51]. In this case the parameters are airspeed, V, and flight path angle, γ. The equilibrium surface approximation (and hence the LPV model) is third order in the parameters and generated at the bifurcation point shown in Figure 5 (a). The 'other' equilibria, shown in Figure 5 (b) are obtained from the cubic approximation and displayed in the figure with the true equilibrium curve.

Analysis shows that the LPV system is uncontrollable at the bifurcation point, but controllable at points arbitrarily near the bifurcation point. Furthermore, controllability degrades as the bifurcation point is approached. To see this, the controllability matrix is evaluated and its minimum singular value is computed at each of the points shown in Figure 5. The results are shown in Table 1, with the bifurcation point shown in bold typeface. As explained in [51], parameterization of

Table 1 Degree of Controllability

s_1	s_2	V	δ_e	σ_{min}
0.010000	0.00	83.7759	-16.4569	0.00186924
0.005000	0.00	83.3882	-18.3686	0.00098419
0.001000	0.00	83.2658	-20.1175	0.00022455
-0.000104	**0.00**	**83.2599**	**-20.6466**	**0.00000000**
-0.000500	0.00	83.2607	-20.8418	0.00008107
-0.006500	0.00	83.4491	-24.2201	0.00153969
-0.010000	0.00	83.7040	-26.6229	0.00276331

the equilibrium manifold around singular points requires replacement of the physical parameters by suitable coordinates on the manifold. The variables s_1, s_2 in Table 1 denote the coordinates used herein. Fixing $s_2 = 0$ and varying s_1 produces a slice through the surface corresponding to fixed γ and varying V.

Even though the system fails to be linearly controllable at the bifurcation point it is locally (nonlinearly) controllable in the sense that the controllability distribution has full generic rank around the bifurcation point. The implication is that any stabilizing feedback controller would certainly be nonlinear and probably nonsmooth.

C. Remarks on recovery from stall

The GTM appears to be remarkably stable. In the coordinated turn illustrated above, the stall speed is about 85 ft/sec. With the controls fixed at their stall equilibrium values the aircraft enters a deep spiral and dives. After several seconds into the departure the controls are reset to their stable 90 ft/sec values. Figure 6 shows the recovery when the controls are reset after 10 seconds. This was intended as an experiment to determine if the vehicle dynamics would permit recovery. No assessment was made as to whether this is an acceptable strategy. In particular structural integrity was not evaluated although it appears that peak acceleration is less than 2 g's. The vehicle drops about 1400 feet.

It is worth noting that the simulations show that recovery can take place even further into the

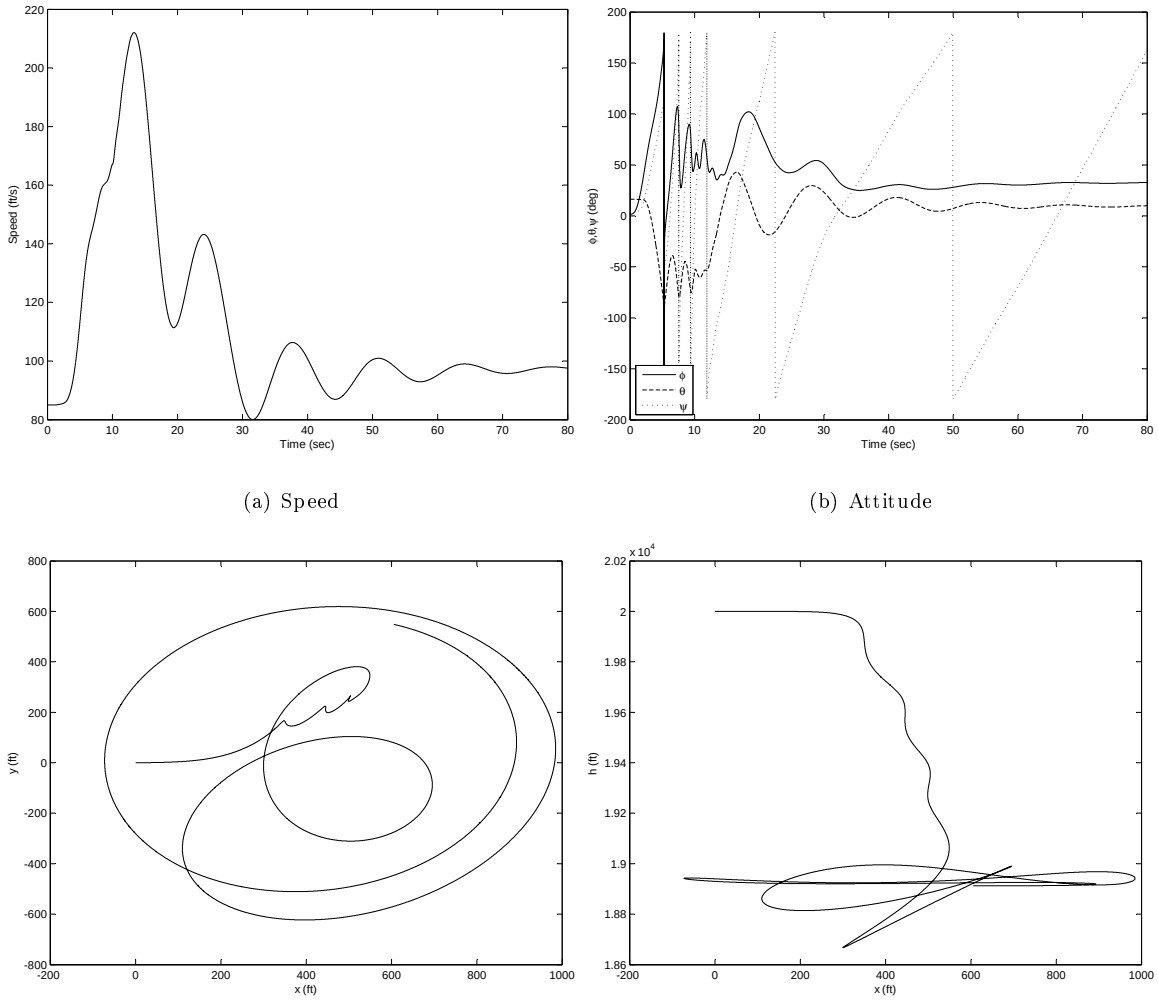

(a) Speed

(b) Attitude

(c) Ground Track

(d) Altitude

Fig. 6 Coordinated turn recovery from stall. The vehicle stalls at about 85 ft/sec during a coordinated turn. After 10 seconds the controls are reset to the 90 ft/sec values. (a) The speed peaks at about 215 ft/sec, 13 sec after stall, before stabilizing at 90 ft/sec. (b) The simulation is carried out using a quaternion representation of attitude, but Euler angles are displayed here. Notice extreme roll before the recovery takes place. (c) The ground track follows the pattern of Figure 3 until the controls are reset. Then it stabilizes into the turn. (d) The aircraft drops about 1400 ft. during the recovery.

departure. Of course, with significantly greater loss of altitude.

VI. Constrained Dynamics

The safe operation of an aircraft requires that certain key variables remain within specified limits. Complicating this is the fact that aircraft are continuously subjected to disturbances and

the control responses are also strictly constrained by actuator limits. The control of systems with state and control constraints is a fundamental problem in control theory that has a substantial literature going back decades, e.g. [10, 52]. In the following paragraphs how this work contributes to our understanding of LOC is considered.

A. Control with state and control constraints

All commercial aircraft are required to respect specified flight envelope restrictions. For example in normal (unimpaired) flight a typical aircraft will have: load factor limitations and also attitude (pitch and roll) and speed limitations. Indeed most aircraft employ some form of envelope protection. The protective actions can range from simple stall warning devices to reshaping pilot commands to actively limiting control actions that would aggravate the situation. These systems present transition issues just like any other switching system. While there is no comprehensive theory of envelope protection, it has been addressed in the literature, for example [16, 17, 53]. An important factor in these controllers is that the control responses are limited. For example, control surfaces have a restricted range of motion and are limited in the control forces that can be generated by them.

Consider a controlled dynamical system

$$\dot{x} = f(x,u), \quad x \in R^n, u \in U \subset R^m \tag{16}$$

where the set U is closed, bounded and convex. Also, suppose the desired envelope is a convex, not necessarily bounded, subset $\mathcal{C}$ of the state space R^n. Feuer and Heyman [10] study the general control problem of interest to us. Specifically, under what conditions does there exist for each $x_0 \in \mathcal{C}$ a control $u(t) \subset U$ and a corresponding unique solution $x(t; x_0, u)$ that remains in $\mathcal{C}$ for all $t > 0$? While some basic results are provided in [10], the general case is unresolved. Concrete results have subsequently been obtained for special cases, especially for linear dynamics with polyhedral constraint sets [8, 9, 19–22, 28, 52]. In the following paragraphs some of the more recent results are applied.

B. The safe set

There are two fundamental issues that need to be addressed: Is it possible to remain within a specified subset of the state space? If so, what control actions are required to insure the aircraft remains within it? These questions have been raised in the literature, for example [8, 9, 28].

Furthermore, suppose that $\mathcal{C}$ is defined by

$$\mathcal{C} = \{x \in R^n \,|\, l(x) > 0\} \tag{17}$$

where $l : R^n \to R$ is continuous. The boundary of $\mathcal{C}$ is the zero level set of l, i.e., $\partial\mathcal{C} = \{x \in R^n \,|\, l(x) = 0\}$. The safe set is defined as the largest positively control-invariant set contained in $\mathcal{C}$. Several investigators have considered the computation of the safe set, the most compelling of which involve solving the Hamilton-Jacobi equation. One of several variants, due to Lygeros [9], is described below.

Consider the operation of the system (16) over a time interval $[0, T]$ for some fixed terminal time $0 < T < \infty$. First, the idea of a controlled invariant set is introduced.

Definition 5. Controlled-Invariant Set A set $\mathcal{I} \subset R^n$ is a controlled-invariant set over a time interval $[t, T]$, if for each $x(t) \in \mathcal{I}$ there exists a control $u(\tau) \in \mathcal{U}$, $\tau \in [t, T]$ such that the solution of (16) emanating from $x(t)$, $\varphi(\tau; x(t), u(\cdot))$, defined on $\tau \in [t, T]$ is entirely contained in $\mathcal{I}$.

This leads to a precise definition of the safe set.

Definition 6. Safe Set Given the envelope $\mathcal{C}$, the safe set is defined as the largest controlled-invariant set on $[t, T]$ contained in $\mathcal{C}$, i.e.,

$$\mathcal{S}(t, \mathcal{C}) = \{x \in R^n \,|\, \exists u(\tau) \subset \mathcal{U}, \forall \tau \in [t, T] : \varphi(\tau; x(t), u(\cdot)) \subset \mathcal{C}\} \tag{18}$$

The main result in [[9]] is the following. Suppose $V(x, t)$ is a viscosity (or, weak) solution of the terminal value problem

$$\frac{\partial V}{\partial t} + \min\left\{0, \sup_{u \in U} \frac{\partial V}{\partial x} f(x, u)\right\} = 0, \quad V(x, T) = l(x) \tag{19}$$

then

$$\mathcal{S}(t, \mathcal{C}) = \{x \in R^n \,|\, V(x, t) > 0\} \tag{20}$$

The function $V(x,t)$ is in fact the 'cost-to-go' associated with an optimal control problem in which the goal is to choose $u(t)$ so as to maximize the minimum value of $l(x(t))$. The function $V(x,t)$ inherits some nice properties from this fact. For instance it is bounded and uniformly continuous. Define the Hamiltonian

$$H(p,x) = \min\left\{0, \sup_{u\in U} p^T f(x,u)\right\} \tag{21}$$

$$\frac{\partial V}{\partial t} + H\left(\frac{\partial V}{\partial x}, x\right) = 0, \quad V(x,T) = l(x) \tag{22}$$

$V(x,t)$ is the unique, bounded and uniformly continuous solution of (19) or (22). Notice that the control obtained in computing the Hamiltonian (21) insures that when applied to each state along any trajectory initially inside of $\mathcal{S}$ the resulting trajectory will remain in $\mathcal{S}$. It follows that this control should be applied for states on its boundary to insure that the trajectory does not leave $\mathcal{S}$.

The envelope defined by (17) can be generalized to an envelope with piecewise continuous boundary. For example, suppose the envelope is defined by

$$\mathcal{C} = \{x \in R^n \,|\, l_i(x) > 0, i = 1,\ldots,K\} \tag{23}$$

Where each of the $l_i(x)$ are continuous functions. Then we need to solve K problems with

$$\mathcal{C}_j = \{x \in R^n \,|\, l_j(x) > 0\}, \quad j = 1,\ldots,K$$

to obtain the largest controlled invariant set in each $\mathcal{C}_j$ and then take their intersection. There are many physical problems in which the tracking of moving boundaries separating to regions of space are important. So it is not surprising that the numerical computation of propagating surfaces is a mature field. The most powerful methods exploit the connection with the Hamilton-Jacobi equation and associated conservation laws; see the survey [54].

Example 3. GTM Phugoid Model Safe Set

The calculation of the safe set for the phugoid model of Section III B will be described. It will be found that the safe set of the intact aircraft is, in fact, the entire envelope. This will not be true for the impaired aircraft. Before proceeding with safe set calculations consider the equilibrium point structure of Equations (4). In essence the aircraft is trimmed at specified values of velocity

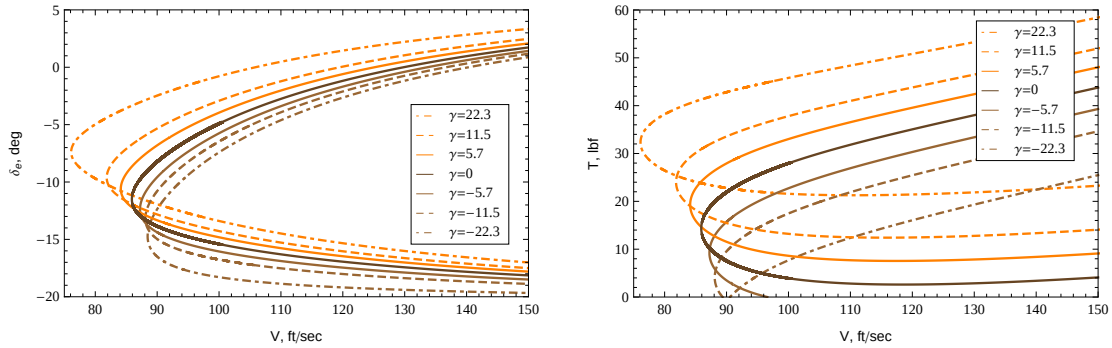

(a) Elevator

(b) Thrust

Fig. 7 Phugoid bifurcation curves show the trim values of elevator and thrust for various of velocities. Each curve corresponds to a different value of flight path angle.

and flight path angle. The problem is to compute the required values of elevator position and thrust. The calculations are performed by specifying a value of flight path angle γ and performing a continuation computation with velocity V as the parameter. Thus, the curves in Figure 7 are obtained. There are two important observations. First the predicted bifurcation velocity is close to that predicted with the 6 degree of freedom model (see Figure 5) - although the bifurcation value for the elevator is significantly different. Examination of the trim values for thrust indicate that there are points in the safe set that are not equilibrium points. In particular, for flight path angles below about -0.15 rad there are admissible velocities above which the aircraft cannot be trimmed with nonnegative thrust.

Figure 8 shows the safe set, $\mathcal{S}$ for unimpaired and impaired aircraft. As expected, the safe set shrinks when the aircraft is impaired. The points in $\mathcal{C}\backslash\mathcal{S}$ produce trajectories that exit the envelope. With limited control authority the safe set is reduced in the lower left quadrant of Figure 8 because at slower speeds, even with the application of both maximum thrust and elevator deflection, it is not possible to generate enough lift to prevent the aircraft from descending along an unacceptably low flight path angle and leaving the prescribed envelope $\mathcal{C}$. In the case where the elevator is jammed, the safe set is reduced in the upper right quadrant of Figure 8 (c) where the higher speeds cause excessive lift to be generated forcing the aircraft to ascend along a flight path angle which exceeds the upper bound of $\mathcal{C}$.

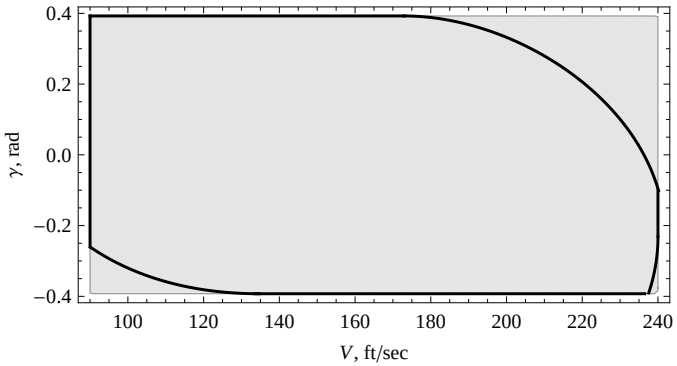

Fig. 8 Safe set with various levels of elevator impairment. For the unimpaired aircraft, in which case the elevator position ranges from -40 deg (-0.698 rad) to +20 deg (0.349 rad), the safe set is the entire envelope (the shaded region). When the elevator is motion restricted in the positive direction to + 3 deg, the safe set contracts somewhat in the bottom left corner (low speed descent) as shown. With elevator jammed at 3 deg the safe set contracts on the right (high speed) as well – marginally at the bottom (descent), but quite significantly at the top (ascent). The safe set for the jammed case is the subset of the flight envelope bounded by the black curve.

VII. Maneuverability

Diminished maneuverability is a central aspect of LOC - whether due to impairment of the aircraft or its entry into an unfavorable flight regime. Maneuverability performance is usually assessed by evaluating an aircraft's capability to perform certain basic tasks under a variety of conditions. Such tasks – including wings level climb and descent, coordinated turns, pull-ups and push-downs – correspond to *steady-state* or *equilibrium* motions in an appropriate mathematical setting. The vehicle must be able to transition between these steady motions.

In earlier work [4] an approach to investigating steady motions of aircraft by examining the equilibrium point structure of a regulator problem associated with the desired motion was introduced. Bifurcation surfaces in multi-parameter problems were identified and bifurcation points were linked to structural instability of the zero dynamics. The limits imposed on the ability of a vehicle to perform a maneuver where thereby associated with both the absence of appropriate equilibria for certain parameter values and also with the difficulty to regulate the vehicle when operating near the bifurcation sets. These ideas were further developed and applied in several papers including

[44, 46, 55]. A somewhat similar approach was recently given by Goman et al [56], referred to therein as a *constrained trim formulation*. The stability of each equilibrium point is evaluated but no connections are made to control system properties as advocated in [4].

A. Basic Steady Maneuvers of Rigid Aircraft

For commercial aircraft the most basic and important steady motions are:

1. straight, level, climbing and descending flight,

2. coordinated turns, level, climbing and descending

In [46] a continuation method was used to examine these motions specifically for the GTM. The limits imposed on these motions by stall bifurcation points were studied and the control system behavior around these points was examined. Using the results of [4] it was argued that regulated flight near stall is difficult because of the structurally unstable zero dynamics.

Of course, not all points identified in a continuation computation are feasible trim conditions. Equilibria with control values outside of the control restraint set need to be excluded. This obvious fact has significant implications as shown below.

Generally the set of viable trim points, $\mathcal{T}$, is viewed in the state-control-parameter space, $\mathcal{X} \times \mathcal{U} \times \mathrm{M} \subset R^{n+m+k}$. Typically, the set of trim conditions is a smooth k-dimensional submanifold of this $n+m+k$-dimensional manifold. It is common practice in bifurcation theory to project $\mathcal{T}$ onto the parameter space M. The result is the bifurcation picture. The folds of $\mathcal{T}$ project onto M as $k-1$-dimensional submanifolds of M. So they partition M into k-dimensional disjoint regions. Each region contains a distinct number of trim points.

If $\mathcal{T}$ is projected onto the n-dimensional state space $\mathcal{X}$ the result is a k-dimensional subset (possibly quite complex) of $\mathcal{X}$ that is also partitioned into subsets by the folds of $\mathcal{T}$. Again each subset is associated with a distinct number of trim points. The significance of this is that the process identifies the possible trim states and the number of trim points associated with each such state. This is important for control analysts and designers concerned with state to state transitions.

Example 4. GTM Phugoid Model Trim Points It is expected that since the unimpaired aircraft has two independent controls and only two states that every point in the envelope could

be made an equilibrium point by proper choice of control. The only issue is that the controls are bounded. However, the situation is more complicated than that. In fact, in this case there may be zero, one and sometimes two admissible control pairs for which each point in the state space can be made an equilibrium point. To understand the maneuverability issues, first compute the values of the controls (T, δ_e) required to force an arbitrary point (V, γ) to be an equilibrium point.

Notice in Figure 7 that most of the curves indicate that there are two trim conditions within the allowed range of flight path angle and airspeed – one normal and one high angle of attack – associated with specific values of thrust, T, and elevator position, δ_e. However, not all are viable because the control values are beyond the permissible range. There are several implications of the control bounds. First, the major effect of the zero thrust lower bound is elimination of normal trims for low speed, sufficiently steep descending flight paths. On the other hand, the 40 lbf thrust upper bound eliminates high angle of attack trims for most ascending flights at sufficiently high airspeeds. For the range of flight path angle and airspeed considered, the normal elevator range does not restrict trim. However, for an elevator range restricted to $+3$ degrees, notice that normal trims are not achievable at higher airspeed. It is worth noting that the range of flight path angles shown for the GTM example is larger than the ± 10 deg that is normal for a typical transport aircraft. Also, the feasibility and value of high angle of attack trims in abnormal situations needs further consideration.

The situation is summarized in Figure 9. Maneuvering from one point to another can be difficult if it requires a transition from normal to high angle of attack trim (or vice-versa). Such a situation could occur, for example, if it is desired to increase the rate of descent at low speeds. Recall that a change from normal to high angle of attack trim requires a significant increase in throttle and is associated with elevator reversal as described in Section IV. The pilot (or auto-pilot) has to recognize the need to change control strategy accordingly. Of course, this picture is altered in significant ways if flaps, spoilers and even landing gear are deployed. In the restricted elevator case shown in Figure 9 the elevator range of motion is limited in the positive direction to 3 degrees. This severely limits the region of normal flight trim.

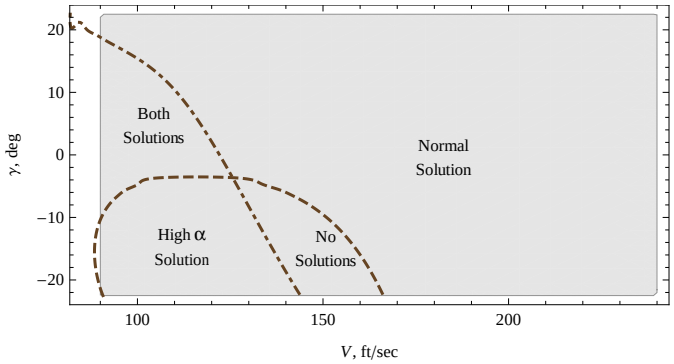

(a) Unimpaired

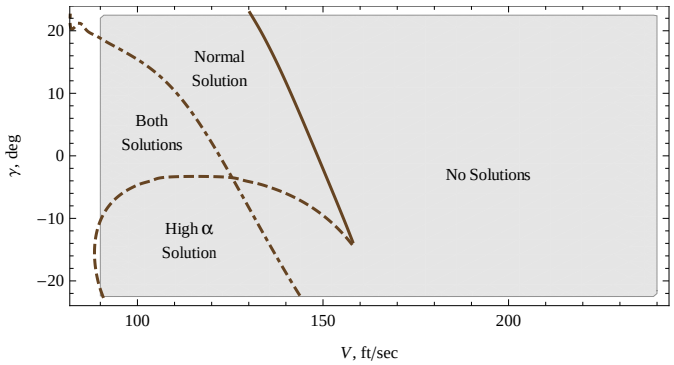

(b) Restricted Elevator

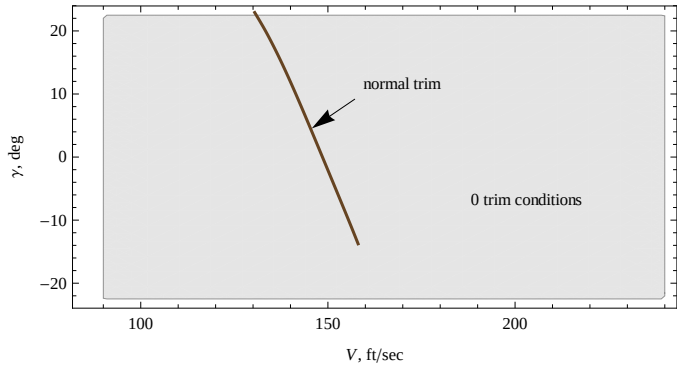

(c) Jammed Elevator

Fig. 9 The viable trim points are identified for the aircraft in unimpaired and impaired configurations. Some states (V, γ) in the flight envelope can be made an equilibrium point by proper selection of admissible control pairs (T, δ_e). At some states, there are two admissible trim conditions and at others only one or none at all.

VIII. Conclusions

In conclusion, the study of an aircraft's equilibrium point structure and the associated control and regulation properties provide direct links between pilot loss of control experience and analytical

flight mechanics. The concepts, methods and tools for performing such studies are presented in this paper. Their application is illustrated using NASA's Generic Transport Model. The trim conditions employed in the examples are straight, wings level flight with specified airspeed and flight path angle or a coordinated turn with specified airspeed, turn rate and flight path angle. The existence of normal and high angle of attack trim points are illustrated as are the differences in the associated piloting requirements. The effect of actuator impairment on the safe set boundary and the trim points within it are also illustrated.

When operating near critical points of the trim equations (i.e., near stall), control properties of the aircraft can change fundamentally with small changes in the aircraft state or parameters. Thus, a small disturbance can cause a dramatic change in how an aircraft responds to pilot inputs. Consequently, regulating an aircraft near stall presents a significant challenge even to experienced pilots. Beyond the critical points themselves, they organize a complex trim point structure throughout the entire flight envelope and, most importantly, within the safe set. For each specified *trim condition* there may be zero, one or more corresponding pairs of admissible state and control values, called *viable trim points*. A unique strategy is typically required to regulate around each distinct trim point corresponding to a particular trim condition. Consequently, the pilot choice of trim point (e.g., normal or high angle of attack trim) to meet a target trim specification (e.g., level flight at a specified airspeed and flight path angle) will impose specific regulating requirements. The pilot needs to be aware of this. In the event of a control impairment, e.g., engine loss or control surface restriction, some of these trim points may may disappear. Thus, to maintain a particular trim condition, the pilot may need to change to an alternate trim point which will typically require a corresponding change in piloting strategy. If the pilot is unaware of the need to switch control strategy a loss of control event might be precipitated.

Appendix I – The GTM 6 Degree-of-Freedom Model

The model used here for all of our examples is derived from an early model of the GTM simulation model (V09.03). Since we made certain simplifications and the GTM model is regularly revised and improved we summarize the details of the model used herein.

$$C_X = -0.0390905 + 0.35218\alpha + 5.36708\alpha^2 - 23.1537\alpha^3 - 26.2264\alpha^4 + 109.938\alpha^5$$
$$+\frac{q\left(2.46995+24.4028\alpha+58.4581\alpha^2\right)\bar{c}}{2V} + 0.125409\alpha\delta_e + 0.0857469\alpha^3\delta_e - 0.00961977\alpha^5\delta_e$$
$$-0.0811392\delta_e^2 + 0.0405696\alpha^2\delta_e^2 - 0.0033808\alpha^4\delta_e^2 - 0.389796\alpha\delta_e^3 + 0.064966\alpha^3\delta_e^3 - 0.0032483\alpha^5\delta_e^3$$

$$C_Y = -1.0499\beta + 0.254159\beta^3 + \frac{r\left(0765433+010909\alpha+0.553414\alpha^2\right)\bar{b}}{2V}$$
$$+\frac{p\left(1.22326\alpha+1.26322\alpha^2-39.4599\alpha^3\right)\bar{b}}{2V} + 0.175591\delta_r$$

$$C_Z = -0.0261857 - 5.38662\alpha + 0.339087\alpha^2 + 28.0138\alpha^3 - 23.0418\alpha^4 - 12.8899\alpha^5$$
$$+\frac{q\left(-28.2259-62.5918\alpha-460.841\alpha^2\right)\bar{c}}{2V} - 0.445354\delta_e - 0.0972682\alpha^2\delta_e + 0.0347678\alpha^4\delta_e$$
$$-0.0811392\alpha\delta_e^2 + 0.0135232\alpha^3\delta_e^2 - 0.00067616\alpha^5\delta_e^2 + 0.389796\delta_e^3 - 0.194898\alpha^2\delta_e^3 + 0.0162415\alpha^4\delta_e^3$$

$$C_L = -0.126318\beta - 0.22119\alpha\beta + 0.255338\beta^3 - 0.191268\beta^5 + \frac{r\left(0.0608527+0.730792\alpha+2.90179\alpha^2\right)\bar{b}}{2V}$$
$$+\frac{p\left(-0.414849-0.325859\alpha+6.67529\alpha^2+125.613\alpha^4\right)\bar{b}}{2V} - 0.0247139\delta_a + 0.0193176\delta_r$$

$$C_M = 0.181738 - 1.10553\alpha - 15.1134\alpha^4 + \frac{q\left(-47.6756+69.4945\alpha+308.277\alpha^2\right)\bar{c}}{2V} - 1.76253\delta_e - 0.920542\alpha\delta_e^2$$
$$+1.35544\delta_e^3 + \left(-0.0261857 - 5.38662\alpha + 0.339087\alpha^2 + 28.0138\alpha^3 - 23.0418\alpha^4\right)\left(-x_{\text{cg}} + \bar{x}_{\text{cg}}\right)$$
$$\left(-12.8899\alpha^5 + \frac{q\left(-28.2259-62.5918\alpha-460.841\alpha^2\right)\bar{c}}{2V} - 0.445354\delta_e - 0.0972682\alpha^2\delta_e\right)\left(-x_{\text{cg}} + \bar{x}_{\text{cg}}\right)$$
$$\left(+0.0347678\alpha^4\delta_e - 0.0811392\alpha\delta_e^2 + 0.0135232\alpha^3\delta_e^2 - 0.00067616\alpha^5\delta_e^2\right)\left(-x_{\text{cg}} + \bar{x}_{\text{cg}}\right)$$
$$\left(+0.389796\delta_e^3 - 0.194898\alpha^2\delta_e^3 + 0.0162415\alpha^4\delta_e^3\right)\left(-x_{\text{cg}} + \bar{x}_{\text{cg}}\right)$$

$$C_N = 0.202546\beta - 0.143331\beta^3 + \frac{r\left(-0.379639-0.205145\alpha-0.937344\alpha^2\right)\bar{b}}{2V}$$
$$+\frac{p\left(-0.00731187-0.45033\alpha+0.724553\alpha^2+16.4433\alpha^3\right)\bar{b}}{2V} - 0.112626\delta_r - 0.000470559\beta\delta_r$$
$$-\frac{1}{\bar{b}}\bar{c}\left(-1.0499\beta + 0.254159\beta^3 + \frac{r\left(0.765433+0.10909\alpha+0.553414\alpha^2\right)\bar{b}}{2V}\right)\left(-x_{\text{cg}} + \bar{x}_{\text{cg}}\right)$$
$$-\frac{1}{\bar{b}}\bar{c}\left(\frac{p\left(1.22326\alpha+1.26322\alpha^2-39.4599\alpha^3\right)\bar{b}}{2V} + 0.175591\delta_r\right)\left(-x_{\text{cg}} + \bar{x}_{\text{cg}}\right)$$

Dedication

This paper is dedicated to Dr. Celeste Belcastro whose enthusiasm for this work and contributions to its formative ideas remains an inspiration to all of us.

Acknowledgement

This research was supported by the National Aeronautics and Space Administration under Contract numbers NNX09CE93P and NNX10CB28C.

References

[1] Ranter, H., "Airliner Accident Statistics 2006," http://www.aviation-safety.net/pubs/[retrieved May 15, 2008], 2007.

[2] Lambregts, A. A., Nesemeier, G., Wilborn, J. E., and Newman, R. E., "Airplane Upsets: Old Problem, New Issues," *AIAA Modeling and Simulation Technologies Conference and Exhibit*, AIAA Paper 2008-6867, Honolulu, Hawaii, 2008.

[3] Wilborn, J. E. and Foster, J. V., "Defining Commercial Aircraft Loss-of-Control: a Quantitative Approach," *AIAA Atmospheric Flight mechanics Conference and Exhibit*, AIAA Paper 2004-4811, Providence, Rhode Island, 16-19 August 2004.

[4] Kwatny, H. G., Bennett, W. H., and Berg, J. M., "Regulation of Relaxed Stability Aircraft," *IEEE Transactions on Automatic Control*, Vol. AC-36, No. 11, 1991, pp. 1325–1323.

[5] Kwatny, H. G., Chang, B. C., and Wang, S. P., "Static Bifurcation in Mechanical Control Systems," *Chaos and Bifurcation Control: Theory and Applications*, edited by G. Chen, Springer-Verlag, 2003.

[6] Berg, J. M. and Kwatny, H. G., "Unfolding the Zero Structure of a Linear Control System," *Linear Algebra and its Applications*, Vol. 235, 1997, pp. 19–39.

[7] Russell, P. and Pardee, J., "Joint Safety Analysis Team- CAST Approved Final Report Loss of Control JSAT Results and Analysis," Tech. rep., Federal Aviation Administration: Commercial Airline Safety Team, December 2000.

[8] Oishi, M., Mitchell, I. M., Tomlin, C., and Saint-Pierre, P., "Computing Viable Sets and Reachable Sets to Design Feedback Linearizing Control Laws Under Saturation," *45th IEEE Conference on Decision and Control*, IEEE, San Diego, 2006, pp. 3801–3807.

[9] Lygeros, J., "On Reachability and Minimum Cost Optimal Control," *Automatica*, Vol. 40, 2004, pp. 917–927.

[10] Feuer, A. and Heymann, M., "Ω-Invariance in Control Systems with Bounded Controls," *Journal of Mathematical Analysis and Applications*, Vol. 53, 1976, pp. 26–276.

[11] Foster, J. V., Cunningham, K., Fremaux, C. M., Shah, G. H., Stewart, E. C., Rivers, R. A., Wilborn, J. E., and Gato, W., "Dynamics Modeling and Simulation of Large Transport Aircraft in Upset Condi-

tions," *AIAA Guidance, Navigation, and Control Conference and Exhibit*, AIAA Paper 2005-5933, San Francisco, CA, 15-18 August 2005.

[12] Murch, A. M. and Foster, J. V., "Recent NASA Research on Aerodynamic Modeling of Post-Stall and Spin Dynamics of Large Transport Aircraft," *45th AIAA Aerospace Sciences Meeting and Exhibit*, AIAA Paper 2007-0463, Reno, NV, 8-11 January 2007.

[13] Jordan, T., Langford, W., Belcastro, C., Foster, J., Shah, G., Howland, G., and Kidd, R., "Development of a Dynamically Scaled Generic Transport Model Testbed for Flight Research Experiments," *AUVSI Unmanned Unlimited*, Arlington, VA, 2004.

[14] Belcastro, C. and Foster, J. V., "Aircraft Loss of Control Accident Analysis," http://ntrs.nasa.gov/archive/nasa/casi.ntrs.nasa.gov/20100030600_2010032989.pdf[retrieved February 10, 2012], 23 July 2010.

[15] Hossain, K. N., Sharma, V., Bragg, M. B., and Voulgaris, P. G., "Envelope Protection and Control Adaptation in Icing Encounters," *41st AIAA Aerospace Sciences Meeting and Exhibit*, AIAA Paper Number 2003-0025, Reno, Nevada, 6-9 January 2003.

[16] Unnikrishnan, S. and Prasad, J. V. R., "Carefree Handling Using Reactionary Envelope Protection Method," *AIAA Guidance, Navigation and Control Conference and Exhibit*, AIAA Paper 2006-6219, Keystone, CO, 21-24 August 2006.

[17] Well, K. H., "Aircraft Control Laws for Envelope Protection," *AIAA Guidance, Navigation and Control Conference*, AIAA Paper 2006-6056, Keystone, Colorado, 21-24 August 2006.

[18] "Airbus Flight Control Laws," http://www.airbusdriver.net/airbus_fltlaws.htm [Retrieved July 10, 2011].

[19] Blanchini, F., "Feedback Control for Linear Time-Invariant Systems with State and Control Bounds in the Presence of Uncertainty," *IEEE Transactions on Automatic Control*, Vol. 35, No. 11, 1990, pp. 1231 – 1234.

[20] Bitsoris, G. and Vassilaki, M., "Constrained Regulation of Linear Systems," *Automatica*, Vol. 31, No. 2, 1995, pp. 223–227.

[21] Bitsoris, G. and Gravalou, E., "Comparison Principle, Positive Invariance and constrained regulation of Nonlinear Systems," *Automatica*, Vol. 31, No. 2, 1995, pp. 217–222.

[22] ten Dam, A. A. and Nieuwenhuis, J. W., "A Linear programming Algorithm for Invariant Polyhedral Sets of Discrete-Time Linear Systems," *Systems and control Letters*, Vol. 25, 1995, pp. 337–341.

[23] Kwatny, H. G. and Blankenship, G. L., *Nonlinear Control and Analytical Mechanics: a computational approach*, Control Engineering, Birkhauser, Boston, 2000.

[24] Morelli, E. A., "Global Nonlinear Aerodynamic Modeling Using Multivariate Orthogonal Functions," *Journal of Aircraft*, Vol. 32, No. 2, 1995, pp. 270–277.

[25] Morelli, E. A. and DeLoach, R., "Wind Tunnel Database Development using Modern Experiment Design and Multivariate Orthogonal Functions," *41st AIAA Aerospace Sciences Meeting and Exhibit*, AIAA Paper 2003-0653, Reno, NV, January 2003.

[26] Lanchester, F. W., *Aerodonetics*, Constable and Company, London, 1908.

[27] Anonymous, "Aircraft Accident Report – United Airlines Flight 232," Tech. Rep. NTSB/AAR-90/06, National Transportation Safety Board, 1990.

[28] Lygeros, J., Tomlin, C., and Sastry, S., "Controllers for reachability specifications for hybrid systems," *Automatica*, Vol. 35, No. 3, 1999, pp. 349–370.

[29] Holleman, E. C., "Summary of Flight Tests to Determine the Spin and Controllability Characteristics of a Remotely Piloted, Large-Scale (3/8) Fighter Airplane Model," Tech. Rep. NASA TN D-8052, NASA Flight Research Center, January 1976.

[30] Jaramillo, P. and Ralston, J., "Simulation of the F/A-18D "Falling Leaf"," *AIAA Atmospheric Flight Mechanics Conference*, AIAA Paper 96-3371, San Diego, July 28-30 1996.

[31] Jaramillo, P., "An Analysis of Falling leaf Suppression Strategies for the F/A-18D," *AIAA Atmospheric Flight Mechanics Conference*, AIAA Paper 96-3370, San Diego, July 28-30 1996.

[32] Croom, M., Kenney, H., Murri, D., and Lawson, K., "Research on the F/A-18E/F Using a 22 percent Dynamically-Scaled Drop Model," *AIAA Atmospheric Flight Mechanics Conference*, AIAA Paper 2000-3913, Denver, 2000.

[33] Young, J., Schy, A., and Johnson, K., "Prediction of Jump Phenomena in Aircraft Maneuvers Including Nonlinear Aerodynamics Effects," *Jounal of Guidance and Control*, Vol. 1, No. 1, 1978, pp. 26–31.

[34] Carrol, J. V. and Mehra, R. K., "Bifurcation of Nonlinear Aircraft Analysis," *Journal of Guidance, Control and Dynamics*, Vol. 5, No. 5, 1982, pp. 529–536.

[35] Guicheteau, P., "Bifurcation Theory Appled to the Study of Control Losses on Combat Aircraft," *Recherche Aerospatiale*, Vol. 2, 1982, pp. 61–73.

[36] Hui, W. H. and Tobak, M., "Bifurcation Analysis of Aircraft Pitching Motions at High Angles of Attack," *Jounal of Guidance and Control*, Vol. 7, 1984, pp. 106–113.

[37] Namachivaya, N. S. and Ariaratnam, S., "Nonlinear Stability Analysis of Aircraft at High Angles of Attack," *International Journal of Nonlinear Mechanics*, Vol. 21, No. 3, 1986, pp. 217–228.

[38] Jahnke, C. C. and Culick, F. E. C., "Application of Bifurcation Theory to High Angle of Attack Dynamics of the F-14 Aircraft," *Journal of Aircraft*, Vol. 31, No. 1, 1994, pp. 26–34.

[39] Goman, M. G., Zagainov, G. I., and Khramtsovsky, A. V., "Application of Bifurcation Methods to Nonlinear Flight Dynamics Problems," *Progress in Aerospace Science*, Vol. 33, 1997, pp. 539–586.

[40] Charles, G. A., Lowenberg, M. H., Wang, X. F., Stoten, D. P., and Bernardo, M. D., "Feedback Stabilised Bifurcation Tailoring Applied to Aircraft Models," *International Council of the Aeronautical Sciences 2002 Congress*, 2002, pp. 531.1–531.11.

[41] Lowenberg, M. H., "Bifurcation Analysis of Multiple-Attractor Flight Dynamics," *Philosphical Transactions: Mathematical, Physical and Engineering Sciences*, Vol. 356, No. 1745, 1998, pp. 2297–2319.

[42] Lowenberg, M. H. and Richardson, T. S., "The Continuation Design Framework for Nonlinear Aircraft Control," *AIAA Guidance, Navigation and Control Conference*, AIAA Paper 2001-4100, Montreal, 6-9 August 2001.

[43] Thomas, S., *Reconfiguration and bifurcation in flight controls*, Ph.D. thesis, Drexel University, Philadelphia, December 2004. [Online] http://dspace.library.drexel.edu/handle/1860/385.

[44] Thomas, S., Kwatny, H. G., and Chang, B. C., "Bifurcation Analysis of Flight Control Systems," *IFAC World Congress*, Prague, 2005.

[45] Bajpai, G., Beytin, A., Thomas, S., Yasar, M., Kwatny, H. G., and Chang, B. C., "Nonlinear Modeling and Analysis Software for Control Upset Prevention and Recovery of Aircraft," *AIAA Guidance, Navigation and Control Conference*, AIAA 2008-6657, Honolulu, Hawaii, 18-21 August 2008.

[46] Kwatny, H. G., Dongmo, J.-E. T., Chang, B. C., Bajpai, G., Yasar, M., and Belcastro, C., "Aircraft Accident Prevention: Loss-of-Control Analysis," *AIAA Guidance, Navigation and Control Conference*, AIAA Paper 2009-6256, Chicago, 10-13 August 2009.

[47] Berg, J. and Kwatny, H. G., "An Upper Bound on the Structurally Stable Regulation of a Parameterized Family of Nonlinear Control Systems," *Systems and Control Letters*, Vol. 23, 1994, pp. 85–95.

[48] Berg, J. and Kwatny, H. G., "A Canonical Parameterization of the Kronecker Form of a Matrix Pencil," *Automatica*, Vol. 31, No. 5, 1995, pp. 669–680.

[49] Von Mises, R., *Theory of Flight*, McGraw-Hill Book Company, New York, 1945.

[50] Wonham, W. M., *Linear Multivariable Control: A Geometric Approach*, Springer-Verlag, NY, 3rd ed., 1985.

[51] Kwatny, H. G. and Chang, B. C., "Constructing Linear Families from Parameter-Dependent Nonlinear Dynamics," *IEEE Transactions on Automatic Control*, Vol. 43, No. 8, 1998, pp. 1143–1147.

[52] Glover, J. D. and Schweppe, F. C., "Control of Linear Systems with Set Constrained Disturbances," *IEEE Transactions on Automatic Control*, Vol. 16, No. 5, 1971, pp. 411–423.

[53] Tomlin, C., Lygeros, J., and Sastry, S., "Aerodynamic Envelope Protection using Hybrid Control,"

American Control Conference, Philadelphia, 1998, pp. 1793–1796.

[54] Sethian, J. A., "Evolution, Implementation, and Application of Level Set and Fast Marching Methods for Advancing Fronts," *Journal of Computational Physics*, Vol. 169, 2001, pp. 503–555.

[55] Thomas, S., Kwatny, H. G., and Chang, B. C., "Nonlinear Reconfiguration for Asymmetric Failures in a Six Degree-of-Freedom F-16," *American Control Conference*, IEEE, Boston, MA, June/July 2004, pp. 1823–1829.

[56] Goman, M. G., Khramtsovsky, A. V., and Kolesnikov, E. N., "Evaluation of Aircraft Performance and Maneuverability by Computation of Attainable Equilibrium Sets," *Journal of Guidance, Control and Dynamics*, Vol. 31, No. 2, 2008, pp. 329–339.